AD A053570

Horizontal Shear Surface Waves on a Laminated Composite

by

B. A. Auld

G. S. Beaupre

G. Herrmann

D D C

RECEIVED

MAY 4 1978

B

SUDAM Report No. 78-3

February 1978

DIVISION
OF
APPLIED
MECHANICS

DEPARTMENT
OF
MECHANICAL
ENGINEERING

STANFORD
UNIVERSITY
STANFORD,
CALIFORNIA
94305

REPORT DOCUMENTATION PAGE		READ INSTRUCTIONS BEFORE COMPLETING FORM
1. REPORT NUMBER SUDAM-78-3	2. GOVT ACCESSION NO.	3. RECIPIENT'S CATALOG NUMBER
4. TITLE (and Subtitle) HORIZONTAL SHEAR SURFACE WAVES ON A LAMINATED COMPOSITE.		5. TYPE OF REPORT & PERIOD COVERED INTERIM rept.
		6. PERFORMING ORG. REPORT NUMBER
7. AUTHOR(s) B. A. AULD, G. S. BEAUPRE G. HERRMANN		8. CONTRACT OR GRANT NUMBER(s) N00014-76-C-0054
9. PERFORMING ORGANIZATION NAME AND ADDRESS DIVISION OF APPLIED MECHANICS STANFORD UNIVERSITY STANFORD, CALIFORNIA 94305		10. PROGRAM ELEMENT, PROJECT, TASK AREA & WORK UNIT NUMBERS ONR:474
11. CONTROLLING OFFICE NAME AND ADDRESS OFFICE OF NAVAL RESEARCH DEPARTMENT OF THE NAVY ARLINGTON, VIRGINIA 22217		12. REPORT DATE FEBRUARY 1978
		13. NUMBER OF PAGES 30
14. MONITORING AGENCY NAME & ADDRESS(if different from Controlling Office)		15. SECURITY CLASS. (of this report) UNCLASSIFIED
		15a. DECLASSIFICATION/DOWNGRADING SCHEDULE

16. DISTRIBUTION STATEMENT (of this Report)

APPROVED FOR PUBLIC RELEASE; DISTRIBUTION UNLIMITED

17. DISTRIBUTION STATEMENT (of the abstract entered in Block 20, if different from Report)

18. SUPPLEMENTARY NOTES

19. KEY WORDS (Continue on reverse side if necessary and identify by block number)

COMPOSITES
LAMINATES
WAVE PROPAGATION
SURFACE WAVES
DISPERSION

20. ABSTRACT (Continue on reverse side if necessary and identify by block number)

It is shown that there exists a new class of surface waves with polarization parallel to the surface, like Love waves, that propagates along the free surface of a half-space consisting of a periodically layered composite with layers parallel to the free surface. A method is presented for deriving these horizontally polarized shear wave solutions from plane wave solutions obtained by applying Floquet's Theorem to an infinite periodically layered medium. The different types of surface wave dispersion relations obtained in this way are discussed and the physical significance of two critical points, the conical point and turning point, is noted.

DD FORM 1473 EDITION OF 1 NOV 65 IS OBSOLETE
1 JAN 73
S/N 0102-LF 014-6601

ABSTRACT

It is shown that there exists a new class of surface waves with polarization parallel to the surface, like Love waves, that propagates along the free surface of a half-space consisting of a periodically layered composite with layers parallel to the free surface. A method is presented for deriving these horizontally polarized shear wave solutions from plane wave solutions obtained by applying Floquet's Theorem to an infinite periodically layered medium. The different types of surface wave dispersion relations obtained in this way are discussed and the physical significance of two critical points, the conical point and the turning point, is noted.

1.   Introduction

Figure 1 shows a small section of a periodically layered medium, with two kinds of material layers (shaded and unshaded in the figure) lying perpendicular to the y axis. We will be concerned with wave motion in the yz plane, involving only an x-component of particle displacement. The motion is uniform in the x direction. That is, the waves are of anti-plane strain type (or horizontal shear in seismological terminology). Alternating layers of the medium have different properties, such that a mechanical impedance discontinuity exists at each interface. Because of these impedance discontinuities a time-harmonic wave progressing through the medium experiences multiple reflections. It is well known in many branches of physics that this situation leads to the existence of certain frequency bands (called stop bands) where progressive wave motion normal to the layers does not exist and the displacement amplitude decays exponentially along the normal direction.

The dispersion relation for the waves just described has been discussed in some detail by Delph, Herrmann, and Kaul[1] and exhibits the expected existence of multiple stop bands. However, because the problem in Fig. 1 is 2-dimensional and the stop-band behavior relates only to field variations along the y axis, wave solutions within a stop band exhibit progressive wave motion along z and exponential decay along y . Solutions with exponential decay toward either +y or -y are obtained. This behavior, somewhat reminiscent of a surface wave traveling along z , prompts one to ask the following question. Under what circumstances can a horizontally polarized shear surface wave (analogeous to a Love wave on a substrate with a single slow velocity layer on the surface) exist on the layered substrate obtained by cutting the medium in Fig. 1

along some plane normal to the y-axis and removing the material on one side of this plane? The purpose of this paper is to show that such surface wave solutions always exist, no matter where the traction-free plane is placed within the structure, and to describe a simple method for obtaining these solutions from solutions for the infinite periodic medium. To our knowledge the existence of these surface waves has not previously been described theoretically or observed experimentally.

It will be seen in what follows that these surface waves on periodic substrates have interesting and unusual properties that are quite unique and distinct from those of Rayleigh and Love surface waves. Significant implications of this fact come readily to mind, as will be discussed in the conclusion.

2. Horizontally Polarized Shear Waves in an Infinite Periodically Layered Medium

It is known from Floquet's theorem that any spatially periodic medium admits wave solutions in which the field distribution along the direction of periodicity is a periodic function multiplied by an exponential. In Fig. 1 this statement applies to the y variation of u_x, where $g(y)$ is the required periodic function with period d equal to that of the structure.

The unit cell of a periodic structure is the basic element that repeats to make up the structure. It may be defined in a variety of ways. In Fig. 1, it is chosen to extend from the left-hand end of one shaded section to the left-hand end of the next shaded section. In the coordinate system chosen the Nth unit cell extends from $y = Nd$ to $y = (N+1)d$. A basic consequence of Floquet's theorem is that the elastic field components u_x and

σ_{xy} in one unit cell differ from u_x and σ_{xy} in the next unit cell only by the factor $e^{iK_y d}$. This follows from the expression for u_x in Fig. 1 and the corresponding stress

$$\sigma_{xy} = \mu \frac{\partial u_x}{\partial y} = \mu e^{-i\omega t} \left\{ \frac{\partial}{\partial y} g(y) + iK_y g(y) \right\} e^{iK_y y} e^{iK_z z}. \quad (1)$$

where the expression in curly brackets is also periodic in y with period d.

From the Floquet property stated above and the continuity of u_x and σ_{xy} at the cell boundaries, we find that the field at the right-hand end of the unit cell is related to that at the left-hand end by the multiplicative factor $e^{iK_y d}$. This is stated at the bottom of Fig. 1 for the Nth unit cell, where a "local" coordinate $y_N = y - Nd$ is used. An important result is that the dispersion relation may be obtained by considering only the field equations within the Nth unit cell.

Figure 2 gives general expressions for the displacement field in layers I and II of the Nth unit cell, expressed in terms of local coordinates. The corresponding stress is calculated by noting that

$$\sigma_{xy} = \mu \frac{\partial u_x(y)}{\partial y} = \mu \frac{\partial u_x(y_N)}{\partial y_N} . \quad (2)$$

The shear velocities in layers I and II are V_{sI} and V_{sII} and K_z is the wave number appearing in the Floquet solution. By satisfying the continuity conditions on u_x and σ_{xy} at the interface between layer I and layer II, we can express B_{II} and A_{II} in terms of B_I and A_I. The periodicity conditions at the bottom of Fig. 1 then give two linear equations in the latter variables. Solution of the secular equation gives the dispersion relation between frequency ω and the wave number components K_y and K_z.

This is the problem solved by Delph, Herrmann, and Kaul in reference 1.

A typical dispersion surface is shown in Fig. 3, where the shaded vertical "steps" are stop bands. On these parts of the surface the real part of K_y (shown in the figure) is constant but the imaginary part of K_y (not shown) varies from zero at the stop band edges to a maximum near the middle of the band. It is this imaginary part of K_y that accounts for the exponential decay of the stop band fields in a direction normal to the layers. Solutions exist with decay in either the positive or negative y directions.

Within the stop bands of Fig. 3 the wave fields decay exponentially along y and, by conservation of energy, the average power flow along y must therefore be zero. From this fact we can draw conclusions about the distribution of u_x for a wave in one of the stop bands. Since power flow density is the time average of $\dot{u}_x \sigma_{xy}$, zero average power flow means that u_x and σ_{xy} are in time phase (Fig. 4). It is then easily shown that the coefficients A and B in the field expressions must satisfy the conditions stated in Fig. 5. To understand the significance of this result it is necessary to examine more closely the stop band structure of Fig. 3.

Figure 6 shows the first two stop bands of Fig. 3 graphed in normalized ω and K_z coordinates. Also shown are straight lines corresponding to the shear wave velocities in the fast and slow layers of the unit cell. The real or imaginary character of k in Fig. 5 is determined by position on the graph relative to these fast and slow velocity lines. For fields within the fast layer k is real for values of ω and K_z to

the left of the fast velocity line

$$\frac{\omega}{\sqrt{\mu'/\rho'}} = K_z$$

in Fig. 6. Values of ω and K_z to the right of this line correspond to imaginary k in Fig. 5. This means that the particle displacement distribution $u_x(y_N)$ in the fast layer is sinusoidal in the first case and a combination of cosh and sinh in the second. A corresponding statement relative to the slow velocity line

$$\frac{\omega}{\sqrt{\mu/\rho}} = K_z$$

can be made for the displacement distribution in the slow layer.

Let us now pose the following question. For values of ω and K_z within one of the stop bands in Fig. 6, are there values of y_N for which the stress σ_{xy} is equal to zero? Since

$$\sigma_{xy} = \mu \frac{\partial u_x}{\partial y_N}$$

from Eq. (2) such traction free planes clearly exist when the displacement u_x is a sinusoidal function of y — that is to say, in the fast layer for points to the left of the fast velocity line of Fig. 6 and in the slow layer for points to the left of the slow velocity line. It will be seen below that such traction-free planes may also exist when the displacement is a hyberbolic function of position. So far we have established only that traction-free planes exist for pairs of values of ω and K_z within a

stop band. This is not yet evidence for the existence of a surface wave. However, in the following section a procedure will be demonstrated for selecting pairs ω, K_z such that the traction-free plane remains at the same position in the structure. The relationship thereby obtained between ω and K_z is then the dispersion relation for a surface wave traveling along a free boundary at that particular location. Under these conditions the infinite medium solution satisfies the equations of elasticity and the correct boundary condition at the free boundary, and therefore provides a valid solution to the surface wave problem.

3.   Horizontally Polarized Shear Surface Waves on a Layered Substrate

Returning to Fig. 6, select initially a value of K_z lying in that part of the first stop band to the right of the fast velocity line. In this region the variation of u_x is hyberbolic in the fast layer and trigonometric in the slow layer. This is illustrated in Fig. 7. Now, consider the variation of the displacement distribution within the unit cell shown, as K_z is kept fixed and ω is varied. It is known from reference 1 that the distribution in the slow layer is symmetric at the lower edge of the stop band and antisymmetric at the upper edge. Within the fast layer the symmetries are reversed. This permits one to sketch qualitatively the graphs at the bottom and top of the figure. Then, imposing continuity of u_x and $\mu(\partial u_x / \partial y_N)$ at the slow-fast interface and supposing that the fast layer is stiffer than the slow $(\mu_{fast} > \mu_{slow})$, one easily arrives at the other displacement distributions shown. The traction-free planes can then be identified as the points of zero slope of the function $u_x(y_N)$. It is seen that such planes exist in both layers and that there may be more than one in each layer.

The figure shows displacement distributions for a single unit cell; but recall that the distribution in successive cells differs only by multiples of the factor $e^{iK_y d}$, where K_y is complex within a stop band. Referring to Figs. 3 and 6 we see that, within the first stop band considered here,

$$K_y d = \pi + i (\mathscr{I}m K_y) d$$

Accordingly, the multiplicative factor relating displacements from cell to cell is

$$-e^{-(\mathscr{I}mK_y)d}$$

where $\mathscr{I}m K_y$ is zero at the edges of the stop band and reaches a maximum within the band. From continuity of u_x at the left- and right-hand edges of the unit cell in Fig. 6 we see that the distributions shown correspond to a wave in which the displacement decays from cell to cell toward the left, as indicated by the undulating arrow.

Another feature apparent from Fig. 7 is that, at fixed K_z , the positions of the traction-free planes vary with ω . Suppose we consider the left-hand traction-free plane in the second diagram from the bottom. This corresponds to the second dot from the bottom in the small insert at the upper left of the figure. If we choose a different value of K_z the traction-free plane will have a different position at this same value of ω but, since the position varies continuously, we can always find a new ω such that the plane remains fixed. This procedure can then be

repeated step by step to construct a dispersion relation

$$\omega = f_s(K_z)$$

for the surface wave traveling along the selected traction-free boundary.

Figure 8, taken from reference 2, shows two surface wave dispersion curves obtained by implementing numerically the procedure described in the preceding paragraph. These correspond to two cases, one with the traction-free boundary at an edge of the slow layer and the second with the boundary within the slow layer. As shown, this simple change in structure produces a radical change in the surface wave properties. In case 1 the wave exists for all values of K_z down to $K_z = 0$, but there is a gap between points A and B. The second case has surface wave propagation only to the right of point A. Figure 6 illustrates the physical significance of these critical points. Point A, where the stop band width reduces to zero, is characterized by the fact that the slope of the dispersion surface in Fig. 3 is not uniquely defined. It is called the conical point and is discussed in reference 3. Point B lies on the fast velocity line in Fig. 6 and is therefore the point at which the fast layer distribution at the upper stop band edge changes from trigonometric to hyperbolic.

Figures 9 to 13 give a general classification of the different types of surface wave behavior occurring in the first stop band for different positions of the traction-free surface. Surface waves with other kinds of dispersion characteristics will exist in the higher stop bands of Fig. 3. Families of surface wave dispersion curves with similar features are seen to occur for free planes located in certain regions of the periodic structure. These families are more complete when the top layer of the substrate

is slow than when it is fast, as would be expected from the fact that Love-type surface waves exist in a single layer only when it is slow compared to the substrate.

Figure 9 shows the type of curves obtained when the free boundary is in the lower half of the slow layer. Case 2 of Fig. 8 is a member of this family. All curves start at the conical point A , some terminate on the upper stop band edge at a finite value of K_z , as shown by the top curve in the figure, and some do not. The sequence of changes is indicated by the arrow on the curves and on the traction-free plane in the insert. The direction of decay into the substrate is denoted by the undulating arrow.

The case of a traction-free plane in the upper half of the slow layer is illustrated by Figs. 10 and 11. When the free boundary is at the upper edge of the slow layer the dispersion curve in Fig. 10 starts at the turning point B and extends to $K_z \to \infty$. This is the outer part of Case 1 in Fig. 8. As the position of the boundary plane is moved into the slow layer, the starting point of the curve moves to larger values of K_z . This set of curves corresponds to a free boundary located within the upper quarter of the slow layer. By contrast, the curves in Fig. 11, which correspond to the inner part of Case 1 in Fig. 8, correspond to a free boundary located within the upper half of the slow layer. These curves all extend from $K_z = 0$ to the conical point A .

Figures 12 and 13 correspond to traction-free planes within the fast layer. In Fig. 12 the curves terminate on points A and B and the bottom member of the series (free boundary on the lower edge of the fast layer) corresponds to the top member of the series in Figs. 10 and 11. Curves for a free boundary in the upper half of the fast layer are very limited in extent. They extend between points A and B , but barely

break away from the stop band edge (not visible on the scale of the figure). Since the infinite medium waves that were used to construct all surface wave solutions have very slow decay rates close to the band edges, this particular family of surface waves has very deep penetration into the substrate.

4. Conclusion

The existence of horizontally polarized shear surface waves on a periodically layered substrate has been demonstrated. As illustrated in Figs. 8 − 13, these waves have very distinctive dispersion curves compared with horizontally polarized shear surface waves of the Love type on a substrate with a single slow surface layer. Unlike Rayleigh waves, but like Love waves, these new surface waves have nonlinear frequency versus wave number relations.[4] However, whereas each member of the Love wave spectrum propagates at all frequencies above some critical frequency characteristic of the mode in question, the Floquet surface waves treated here are, in some cases, restricted to a limited frequency range and can exhibit both bandpass and bandstop filter characteristics.

It is not claimed that the solutions presented here are the only possible horizontally polarized shear waves that can exist on a periodically layered substrate. They are however valid solutions, even though developed by first applying Floquet's theorem to the infinite periodic medium, because they satisfy all of the required elasticity equations and boundary conditions.

Since layered composites are finding increasing use in structural applications, these new surface wave solutions are of current importance with regard to vibration problems in layered structures. If, for example,

one is concerned with protecting a delicate instrument from the vibrations generated by a motor mounted on the same structure, one would clearly wish to avoid direct transmission of surface waves from the motor to the instrument. This requirement would therefore impose constraints on the composition of the layered structure so as to avoid efficient surface wave excitation and transmission within the frequency spectrum of the vibrations generated by the motor.

Another fruitful area of potential applications is in electronic filtering and signal processing. Since 1967 both Rayleigh and Love surface waves have been extensively used in various devices of this category, ranging from elaborate processing systems for radar to inexpensive selection filters for TV sets. In many of these devices the surface waves are excited by an array of electrodes deposited on the surface, with spacing equal to one-half of the surface wavelength. These electrodes are then driven electrically with suitable phasing so that they radiate waves constructively along the surface. The electrode spacing, being equal to a half-wavelength, decreases with frequency. This poses a fabrication problem for devices operating at frequencies above 1000 MHz, where one-half of a Rayleigh wavelength is less than one micron. The surface waves of interest in this paper have a unique feature relevant to this practical problem. It will be noted in Fig. 11 that there is wave propagation at finite frequency for all values of K_z down to zero. This is a property not shared by any other type of surface elastic wave. In potential electronics applications its importance stems from the fact that the wavelength $\lambda = (2\pi/K_z)$, becomes larger as K_z becomes smaller. One therefore has a means for obtaining increased surface wavelengths at high frequencies and thereby relieving the fabrication problem noted above.

Furthermore, one may note that the $k_2 = 0$ point is a cut-off for the surface wave; that is, the solution does not exist as a <u>propagating</u> wave below the frequency corresponding to $k_2 = 0$. An extremely interesting question concerns the behavior of the solution at frequencies <u>below</u> this critical frequency. In an ordinary closed waveguide, a propagating mode becomes decaying (or evanescent) at frequencies below cut-off. This type of behavior has never been observed in a surface wave solution and, if it occurs in this case, would constitute another unusual property of this new class of surface waves.

5.   <u>Acknowledgment</u>

References

1. Delph, T. J., Herrmann, G., and Kaul, R. K., to be published.

2. Auld, B. A., Beaupre, G. S., and Herrmann, G., Electronics Letters 13, 525–527 (1977).

3. Delph, T. J., Herrmann, G., and Kaul, R. K., Int. J. Solids and Structures 13, 423–436 (1977).

4. Lardat, C., Maerfeld, C., and Tournois, P., Proc. IEEE 59, 355–368 (1971).

5. White, R. M., IEEE Trans. ED–14, 181–189 (1967).

Figure Captions

Figure 1   Floquet solution for propagation in the infinite periodic structure.

Figure 2   Displacement field distributions in the Nth unit cell, expressed in terms of the local coordinate $y_N = y - Nd$.

Figure 3   Dispersion surface for x-polarized shear wave propagation in an infinite periodically layered medium.

Figure 4   The phase relationship between u_x and σ_{xy} in a stop band.

Figure 5   General particle displacement distribution functions in a stop band.

Figure 6   Detail of the first two stop bands in Figure 3.

Figure 7   Shift in position of the traction-free planes $\sigma_{xy} = 0$ as a function of ω .

Figure 8   Two examples of surface wave dispersion curves for a layered substrate.

Figure 9   Surface wave dispersion curves for a free boundary in the lower half of the slow layer.

Figure 10   Surface wave dispersion curves of the first kind for a free boundary in the upper half of the slow layer.

Figure 11   Surface wave dispersion curves of the second kind for a free boundary in the upper half of the slow layer.

Figure 12   Surface wave dispersion curves for a free boundary in the lower half of the fast layer.

Figure 13   Surface wave dispersion curves for a free boundary in the upper half of the fast layer.

N^{th} Unit Cell

$y_N = 0$ $y_N = d$

$$u_x\big|_{y_N = d} = e^{iK_y d}\, u_x\big|_{y_N = 0}$$

(I)   (II)
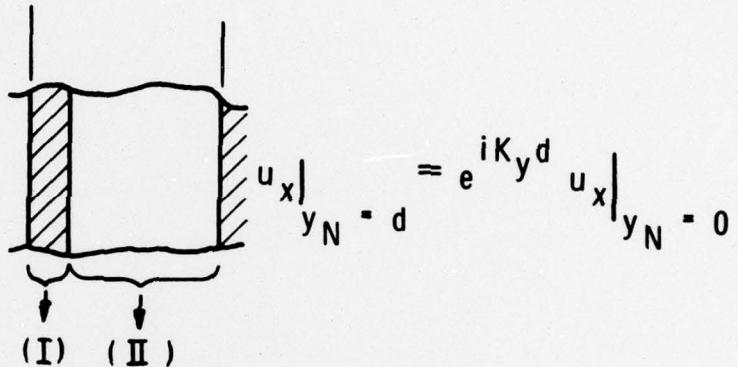
(I) $u_x = e^{iK_z z}\left(A_I e^{ik_I y_N} + B_I e^{-ik_I y_N}\right)$

$$k_I^2 + K_z^2 = \left(\omega/V_{sI}\right)^2$$

(II) $u_x = e^{iK_z z}\left(A_{II} e^{ik_{II} y_N} + B_{II} e^{-ik_{II} y_N}\right)$

$$k_{II}^2 + K_z^2 = \left(\omega/V_{sII}\right)^2$$
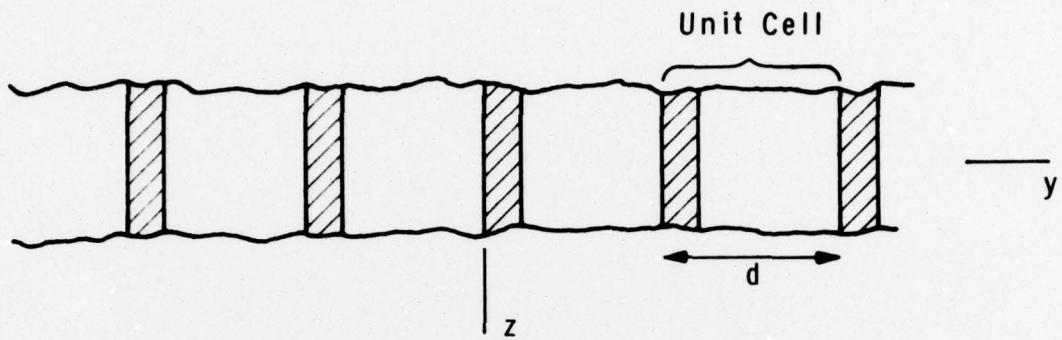
Floquet's Theorem

$$u_x = e^{-i\omega t}\, f(y)\, e^{iK_z z} = e^{-i\omega t}\, g(y)\, e^{iK_y y}\, e^{iK_z z}$$

Period d

In the Nth Unit Cell

$$y_N = y - Nd$$

$$u_x\Big|_{y_N = d} = e^{iK_y d}\; u_x\Big|_{y_N = 0}$$

$$\sigma_{xy}\Big|_{y_N = d} = e^{iK_y d}\; \sigma_{xy}\Big|_{y_N = 0}$$

In a Stop-Band

$$u_x = e^{-i\omega t} e^{iK_z z} \left(A e^{iky_N} + B e^{-iky_N} \right)$$

$$\sigma_{xy} = ik\mu e^{-i\omega t} e^{iK_z z} \left(A e^{iky_N} - B e^{-iky_N} \right)$$

$$\left.\begin{array}{c}\\ \\ \\ \\ \end{array}\right\} \begin{array}{c} \text{In} \\ \text{phase} \end{array}$$

$$k^2 + K_z^2 = \left(\omega / V_s \right)^2$$

k Real

$$|B| = |A|$$

k Imaginary

$$\text{Arg } B = \text{Arg } A + n\pi$$

In a Stop-Band

(Average Power Density)$_y$ = Time Average of $\mathring{u}_x \sigma_{xy}$ = 0

$$\Longrightarrow$$
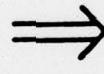
$\mathring{u}_x$ and σ_{xy} are 90° out of time phase

and

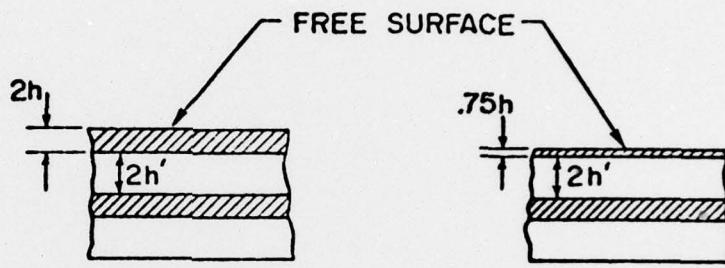u_x and σ_{xy} are in phase

ω

Kz
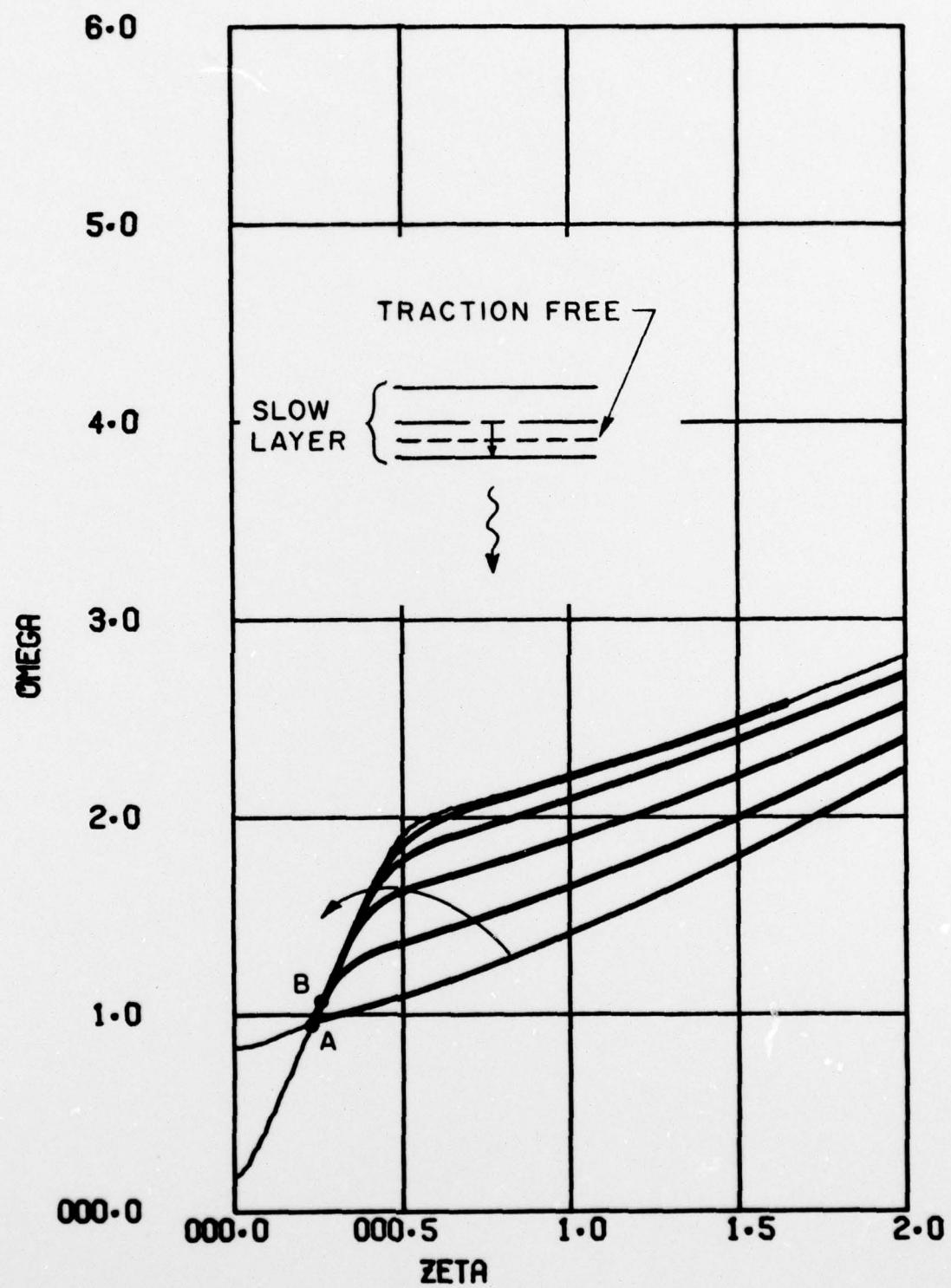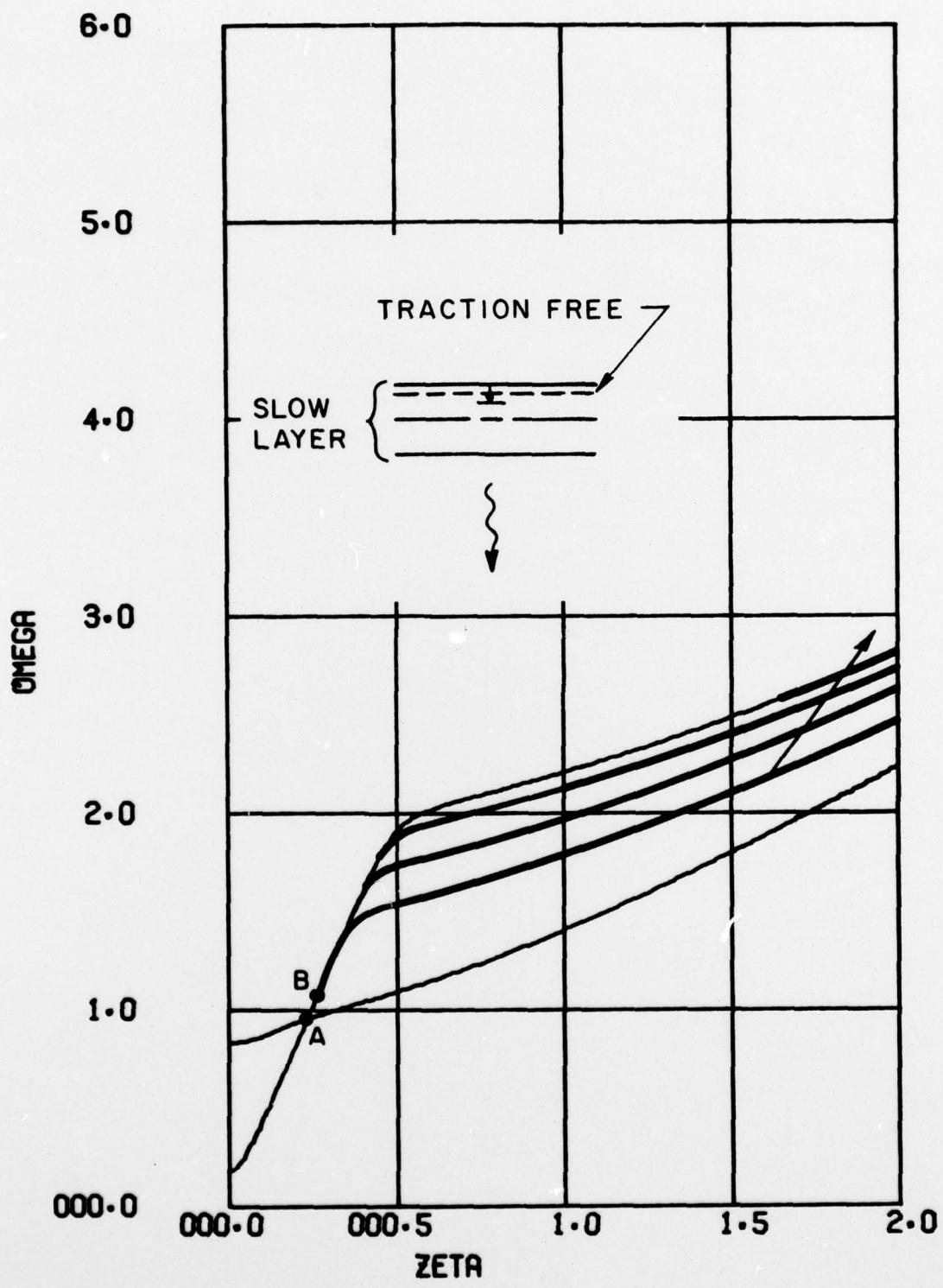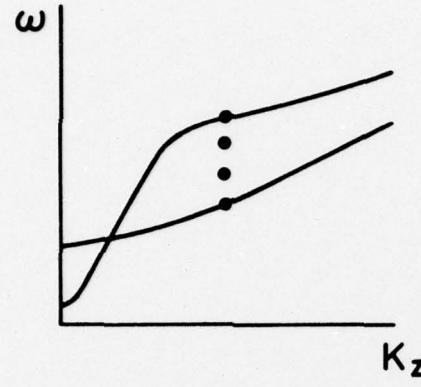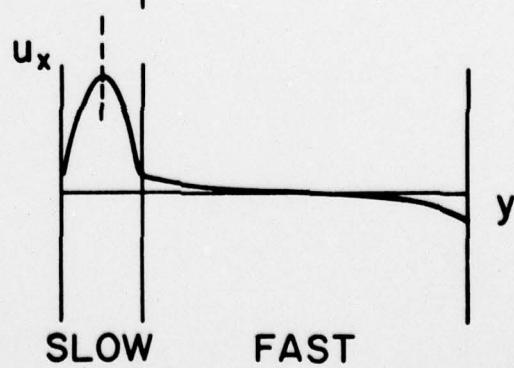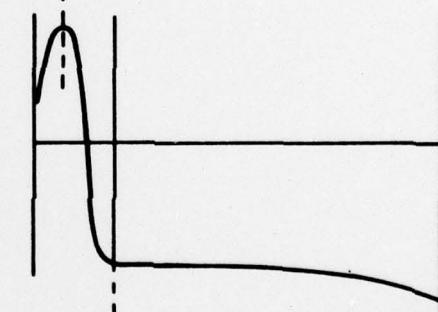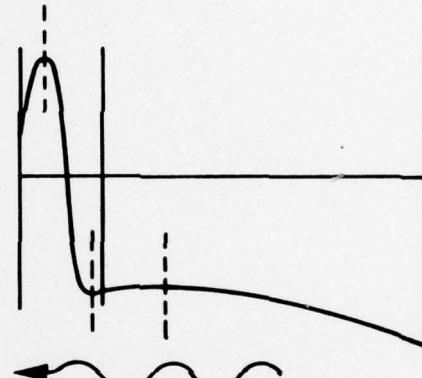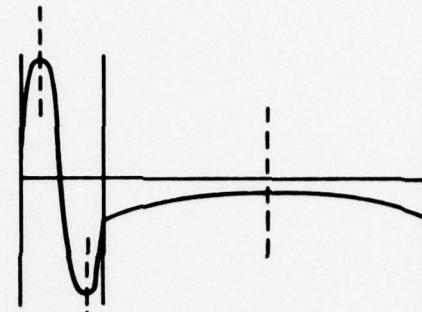
ω
INCREASING

---- TRACTION - FREE
PLANES

uₓ

y

SLOW   FAST